

An image based multi-angle method for estimating reflection geometries of flexible objects

Aditya Sole¹, Ivar Farup¹, and Shoji Tominaga²;

1. The Norwegian Colour and Visual Computing Laboratory, Gjøvik University College, Gjøvik, Norway,

2. Graduate School of Advanced Integration Science, Chiba University, Chiba, Japan

Abstract

Gonio-spectrometers and multi-angle spectrophotometers are successfully used for performing multi-angle measurements of non-diffuse materials like metallic inks and paints used in the print and packaging industry and car paint industry. Using a gonio-spectrometer to measure the amount of light reflected at different incident and reflection angles is a time consuming and an expensive process and is mainly performed in laboratories for research purposes.

In order to perform multi-angle planar measurements, at relatively cheaper and faster way, we use a geometrical method which can be used with an image based measurement setup to measure such materials. The image based measurement setup help record the light reflected from the sample, in the digital pixel array sensor. The geometrical method estimates the incident (θ_i) and reflection (θ_r) angles at a given point (P) on the sample surface. It also maps the pixel positions on the camera sensor array to the corresponding point (P) on the sample surface. This information can therefore be used to understand the amount of light incident and reflected from a given point (P) on the sample surface and record it accordingly.

The proposed measurement setup can be used in, for example packaging industry, to perform online gonio-metric measurements during material reproduction process and estimate the incident and reflection angles of homogeneous flexible object materials when measuring light incident and reflected from the sample at different angles.

The results obtained show that the geometrical method corrects for the geometrical distortions and estimate the incident (θ_i) and reflection (θ_r) angles successfully.

Introduction

We measure appearance of an object surface with the goal of objectively describing and quantifying our visual impressions with measurement values. Measurements lets us communicate the appearance of an object surface in numerical terms. The overall appearance of an object/material is a combination of its chromatic attributes and its geometric attributes [1].

The appearance of non-diffuse materials like metallic inks, coatings (e.g. varnish, special effect coatings), which are widely used to produce desirable appearance of the products especially in printing and packaging industry, vary with the direction of illumination and viewing. Other materials like gonio-chromatic materials [2] produce a very desirable appearance by exhibiting a shift or change in perceived colour depending upon the illumination and viewing angles [2, 3]. The change/shift in appearance (in terms of perceived colour) is achieved due to varying reflections at differ-

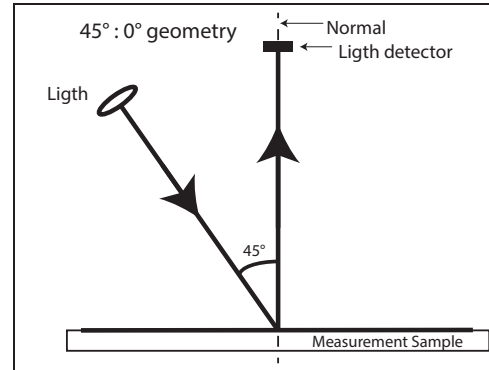


Figure 1. 45°: 0° measurement geometry

ent viewing angles. As we know, when choosing a measurement instrument to be used for measuring these kind of materials, illumination and measurement geometry of the instruments affects the outcome of the measurements [4]. According to Takagi et al. [5], 1485 different geometries are required for characterising the reflection properties of special effect coatings. Storing and using/processing such a huge data is a challenge/serious problem. Therefore, the main goal of Kirchner and Werner's [6] paper was to show that reduction of number of measurement geometries is essential, and can be possible with a physical interpretation of the reflectivity at different measurement geometries.

In traditional colour pigments, part of the incident light is absorbed while the rest is diffusely scattered. The perceived colour from such pigments is therefore independent of the measurement geometry and the traditional single geometry 0°:45° measurements are sufficient to characterise the colour of these coatings. The measurements performed using these instruments, on isotropic diffuse materials, correlate well with what we see [7]. In a 45°:0° geometry the sample is usually lit with light incident at 45° and the reflected light is measured at the normal from the sample surface (0°) (refer Figure 1). In the graphic arts and printing industry, instruments with 0°:45° geometry and vice versa are well known, and are used extensively for measurement of colour [8].

In metallic coatings, the interaction of light with metallic coatings results into specular reflection from the flakes, and the perceived brightness is dependent on the viewing angle and independent of illumination angle. The perceived hue and chroma remain independent of the measurement geometry.

Pearlescent coatings (pearl interference pigments) usually consist of thin metal oxide layers on transparent mica platelets. The hue, chroma and brightness of these coatings are dependent

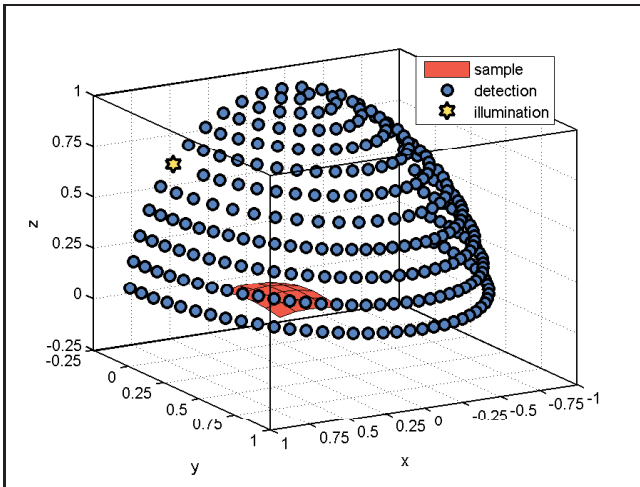


Figure 2. Gonio-metric measurements (Image taken from [14] and is licensed under CC BY-NC-ND)

on both illumination and viewing angles. Therefore, the number of measurement geometries required to measure and characterise pearlescent coatings is greater than for metallic coatings. Nadal and Early [9] proposed a measurement protocol for the accurate colour characterisation of pearlescent interference coatings using an understanding of their scattering mechanism as a guide. A set of measurement geometries were suggested to perform a colorimetric characterisation of pearlescent coatings. These measurement geometries were illumination angles $15^\circ, 45^\circ, 65^\circ$ and aspecular angles $15^\circ, 35^\circ, 45^\circ, 70^\circ$, and 85° for each illumination angle.

Therefore, in order to characterise such materials, they should be measured at more than one illumination/viewing angle combination [2, 10]. Several multi-angle spectrophotometers (e.g. X-rite MA98, BYK-mac, Datacolor Multi FX10) are used for colour measurement and process control during reproduction of such materials [11]. Even if these instruments are commercially available, they are very expensive, measure at fixed illumination and reflection angles and lack standard procedures to perform multi-angle measurements [12].

In this paper we use a geometrical method that can be used with image based measurement setup similar to one proposed by Rong Lu and Kappers [13] to measure such materials at a faster speed. This paper describes a geometrical method to estimate incident (θ_i) and reflection (θ_r) angles along with a measurement setup (using a camera) which can be used to perform planar multi-angle measurements on the above described sample materials, and validates the model with an image clicked of a test sample using the setup and calculates the incident (θ_i) and reflection (θ_r) angles to verify the geometrical method.

Measurement setup and angle estimation model

To perform faster measurements with different incident and reflection angle combinations, we use an image based measurement setup that should help perform measurements of the reflected light at relatively faster speed at different illumination and reflection angles. In the existing measurement setups (e.g.

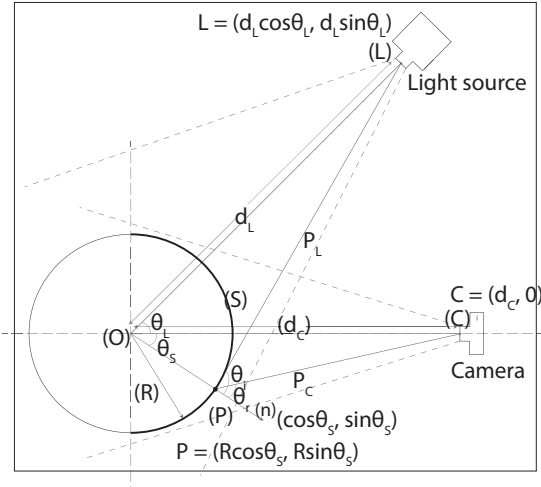


Figure 3. Measurement setup

gonio-spectrometers, multi-angle spectrophotometers), the sample is usually flat on a surface and the light capturing sensor and/or light source rotate/move in the planar angles and azimuthal directions to illuminate and record the reflected light from the sample surface in different directions [14]. These setups therefore requires considerable amount of time to record the reflectance at multiple angles. Figure 2 shows an illustration of measurement angle setup used in some of the existing measurement devices to record multi-angle measurements.

In order to avoid these moving parts (which are main cause of increase in measurement time) and thus reduce the measurement time, in the proposed setup, we keep the light source and the measurement sensor at fixed position from the sample (for example light source at 45° and sensor at 0°) and curve the measurement sample onto a cylinder [13, 15, 16] as shown in the setup (Figure 3). Figure 3 shows the measurement setup we use for capturing the light reflected from a material substrate using an image based device. We therefore, replace the flat surface measurement using gonio-spectrometer with a curved surface observation by a camera in our setup.

Rong Lu and Kappers [13] presented a similar setup and a novel method to measure velvet fabric that is wrapped around a right-circular cylinder and the light reflected from this curved fabric is recorded using a digital CCD camera. They used a wide, uniform and parallel beam light source to irradiate the curved velvet fabric at specified angles. The light reflected (scattered) from the fabric is then detected by a digital camera at a defined angle (usually normal to the sample). This apparatus was capable of measuring radiance of the scattered beam in all angular directions around the cylinder. In our setup we use an uniform point light source to illuminate a curved flexible object (for example packaging sample print) instead of a parallel beam light as used in other setups [13, 16]. Using an uniform point-source illumination should help us have a multiple combination of incident (θ_i) and reflection (θ_r) angle geometries.

Referring to our measurement setup (Figure 3) the semi-circle (S) will be the curved substrate (for example packaging sample print) to be measured. The substrate is curved onto a cylinder of known radius R. Point C is the sensor position (digital camera

sensor in this setup) approximately at the center of the curved sample at a fixed distance d_C . L is a point light source illuminating the sample at a fixed angle $0^\circ < \theta_L < 90^\circ$ at a known distance d_L from the center of the curved sample.

Assuming that the curved sample is homogeneous, light incident and reflected at any given point on the sample will provide information with respect to the light source position (L), camera (C) and the surface normal vector (\mathbf{n}) direction. Figure 3 also shows the setup in a vector plane were θ_i and θ_r are incident and reflection angles with respect to the normal n at a given point P on the curved sample surface.

Considering the setup in a vector plane, θ_i and θ_r can be calculated as given in Equation (1).

$$\cos \theta_i = \frac{\mathbf{P}_L \cdot \mathbf{n}}{|\mathbf{P}_L|} \quad (1)$$

$$\cos \theta_r = \frac{\mathbf{P}_C \cdot \mathbf{n}}{|\mathbf{P}_C|}$$

From the co-ordinate system we know the co-ordinate values for P_L and P_C and n . Inserting the values we can further solve for θ_i and θ_r (refer Equations (2)).

$$\begin{aligned} \mathbf{P}_L &= [(d_L \cos \theta_L - R \cos \theta_S), (d_L \sin \theta_L - R \sin \theta_S)] \\ \mathbf{P}_C &= [(d_C - R \cos \theta_S), (0 - R \sin \theta_S)] \\ \mathbf{n} &= (\cos \theta_S, \sin \theta_S) \\ |\mathbf{P}_L| &= \sqrt{(d_L \cos \theta_L - R \cos \theta_S)^2 + (d_L \sin \theta_L - R \sin \theta_S)^2} \\ |\mathbf{P}_C| &= \sqrt{(d_C - R \cos \theta_S)^2 + (-R \sin \theta_S)^2} \\ \cos \theta_i &= \frac{d_L \cos(\theta_L - \theta_S) - R}{\sqrt{d_L^2 + R^2 - 2d_L R \cos(\theta_L - \theta_S)}} \\ \cos \theta_r &= \frac{d_C \cos \theta_S - R}{\sqrt{d_C^2 + R^2 - 2d_C R \cos \theta_S}} \end{aligned} \quad (2)$$

Where, R is the curved sample radius, d_L is the distance between the curved sample center (O) and light source (L), d_C is the distance between the curved sample center (O) and the camera (C), θ_L is the angle the light source (L) makes with respect to the x axis (which goes through the sample center (O)), θ_S is the angle the given point (P) makes with respect to the x axis (which goes through the sample center (O)), θ_i is the incident angle between the light source (L) and normal (n) on the curved surface at the given point (P), θ_r is the reflection angle between the camera (C) and the normal (n) on the curved surface at the given point (P).

Calculating θ_S

However, as we can see, when choosing a point on the curved sample surface to record the incident and reflected light at different angles (θ_i , θ_r), the θ_S angle changes with change in the location on the curved sample surface. It is therefore important to calculate θ_S for the given point on the curved surface in order to estimate the incident and reflection angles (θ_i , θ_r).

To calculate θ_S , let us refer to the setup (Figure 4) with only the curved sample (S) and the camera (C) at a distance d_C from the center (O) of the curved surface. When using a digital camera array sensor, the point C_L is the point where the light reflected from the curved sample surface enters the camera through its lens setup. The light reflected from the point P on the curved sample surface will therefore be recorded at pixel point A at a physical distance d_A from the center of the camera sensor array $C(O)$ (refer Figure 4). The digital pixel (at distance d_A in millimetres) that corresponds to the given point P on the curved sample surface can be estimated with Equation (3).

$$d_A = \frac{R \sin \theta_S F_L}{d_C - R \cos \theta_S} \quad (3)$$

Where, F_L is the physical focal length of the camera from camera entrance point C_L , R is the curved sample radius, d_C is the distance between the curved sample center (O) and the camera entrance point (C_L) and θ_S is the angle the given point (P) makes with respect to the x axis (which goes through the sample center (O))

Solving Equation (3) for θ_S , the solution being quadratic we get two solutions out of which one is correct,

$$\cos \theta_S = \frac{2d_C R d_A^2 \pm \sqrt{(-2d_C R d_A^2)^2 - 4(R^2 d_A^2 + F_L^2 R^2)(d_C^2 d_A^2 - F_L^2 R^2)}}{2R^2(d_A^2 + F_L^2)} \quad (4)$$

Thus, the calculated θ_S can be used in Equation (2) to estimate the incident and reflection angles at any given point P on the curved surface.

As the sample is curved and commercial digital camera uses a lens setup to focus the incident light on the sensor array, the exact focal length can be difficult to measure and will always depend on the camera used. We therefore calculate the camera focal length in digital pixel values rather than using the focal length information obtained through the raw image file. Section *Effective focal length (F_P)* explains the calculation for the camera focal length in digital pixels in detail. We refer this focal length as effective focal length (F_P).

Effective focal length (F_P)

To calculate the focal length in pixel number we capture the image of the curved sample surface with the digital camera so that the sample covers the maximum field of view of the camera. The curved sample edges can then be detected by using an edge detection algorithm. The sample edges in the image captured will be tangent to the curved sample surface and thus will form a 90° angle with the normal at that point as shown in Figure 4. Using basic SSA (two known sides and a not-included angle) triangle solution we can calculate the corresponding θ_S for the sample edge. We then can calculate the effective focal length (F_P) for the camera.

Re-arranging Equation (3) for calculating F_P ,

$$F_P = \frac{d_P (d_C - R \cos \theta_S)}{R \sin \theta_S} \quad (5)$$

This effective focal length then can be used in Equation (4) as F_L along with digital pixel position d_P as d_A to calculate θ_S for any given point on the curved sample surface.

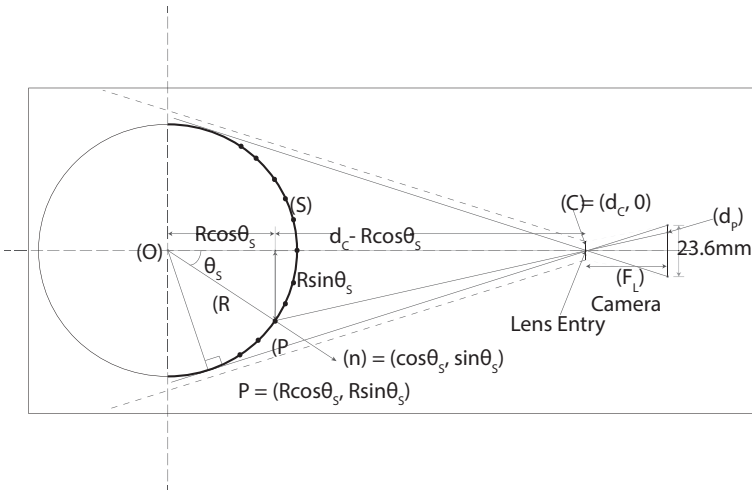


Figure 4. θ_s calculation

Validating the θ_s model

In order to validate the proposed model, a setup consisting of the measurement sample, digital camera, and light source was used. Figure 3 shows the schematic diagram of the setup. The semi-circle is the curved measurement sample. The sample is illuminated at 45° from the normal to the sample, whereas, the digital camera is normal to the sample. A film projector with tungsten light source and Nikon D200 digital camera was used as light source and light capture sensor. To verify the model to calculate θ_s (Equation (4)) a ruler printed on paper substrate was used instead of a non-diffuse coloured sample.

Ruler points (centimetre lines) on the printed ruler should help us locate points (P) on the curved surface for calculating the angle (θ_s) for those points. We understand that the proposed model should

1. correct for geometrical distortion caused due to sample curvature, and lens, as the camera focal length is calculated in digital pixel values using the actual digital pixel points on the camera sensor that correspond to the real objects,
2. and provide the correct pixel location on the sensor (which being flat) that corresponds to the given position on the curved sample surface.

Figure 5 shows the captured image. In order to minimize distortion due to lens, the object is positioned at the centre of the image plane with sufficient distance from all the 4 corners. Unlike Marschner et al. [15]'s method, we use manual physical measurements to determine the incident light position and the camera. In order to find the object position in real space and the corresponding mapping, we use second derivative (only in the horizontal direction (x-axis)) to locate the pixel positions of the ruler points (refer Figure 6) along with the curved sample edge to be used for calculating the effective focal length for the camera using the procedure described in the previous section (using Equation (5)). This calculated effective focal length (F_p) was then used for calculating θ_s angle for the ruler points (P) on the curved surface using Equation (4).

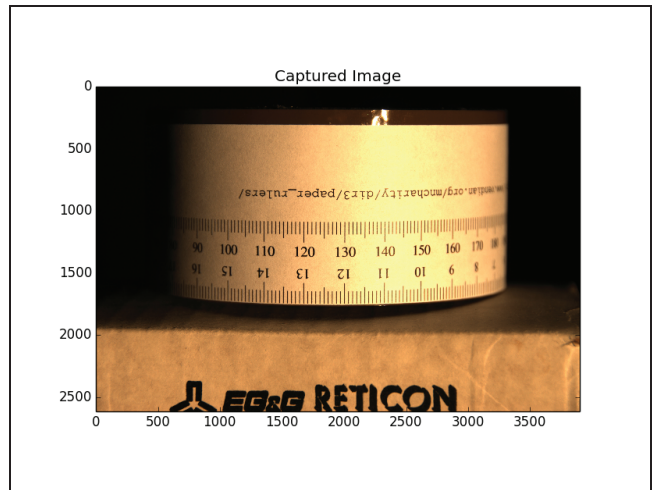


Figure 5. Captured image

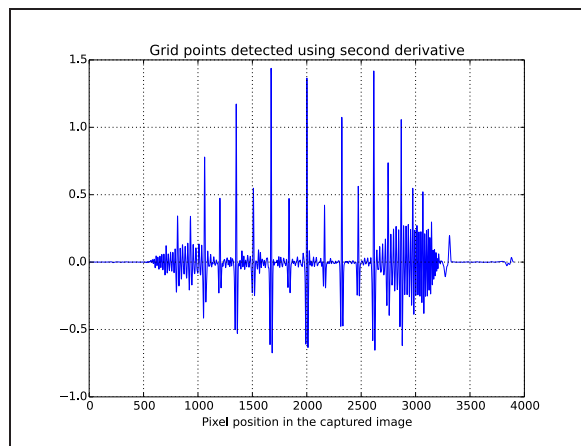


Figure 6. Ruler points

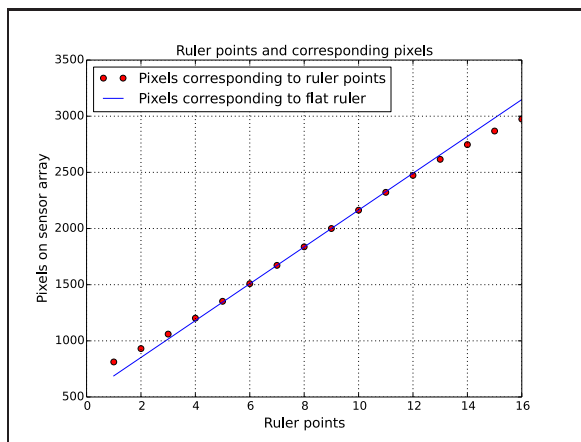


Figure 7. Pixel position in the sensor array against the ruler points

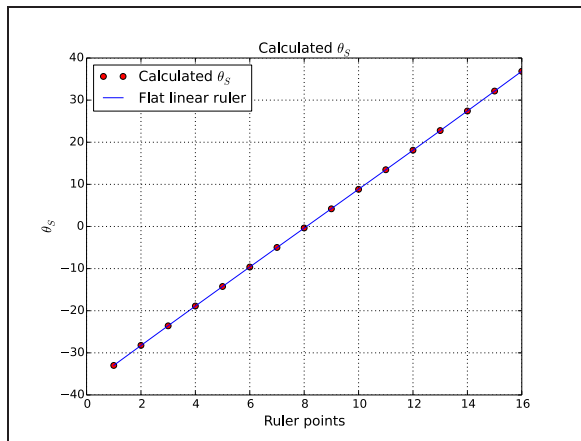


Figure 8. Calculated θ_S against the ruler points

A plot of these calculated angles against the ruler points on the curved sample surface (printed ruler) should give us a straight line at 45° if the model is successfully able to calculate the angle (θ_S). Figure 7 shows the plot for the pixels positions in the sensor array against the ruler points the pixel positions for image of a flat ruler. We can observe that the pixels on sensor array corresponding to the ruler points do not lie on the straight line due to the depth of the ruler as it not being flat. Figure 8 shows the plot for the calculated θ_S against the ruler points and the flat ruler points. From these graphs we can observe that the model (Equation (4)) is able to calculate the angle θ_S for the corresponding ruler points on the curved sample surface and correcting for the geometrical distortion in the image due to the sample curvature (refer Figure 7). These angles (θ_S) can then further be used in Equation (2) to estimate the incident and reflection angles at the corresponding points (P) on the curved sample surface. Pearson's correlation coefficient was calculated between (1) the pixel positions in the sensory array and the ruler points, and (2) calculated θ_S and the ruler points. Pearson's distance was calculated from the correlation coefficients to see how well the model corrects for the geometrical distortion. Pearson's distance (d_r) is defined as $d_r = 1 - r$, where r is Pearson's correlation coefficient. Looking at the ratio between the Persons distances (between (1) and (2)), we can see that the model corrects for geometrical distortion by a factor of 202.6. Table 1 shows the correlations coefficients and

Pearson's correlation coefficient and Pearson's distance

	Pearson's correlation coefficient	Pearson's distance
Calculated θ_S and grid points	0.99999	4.2×10^{-6}
Pixel position and grid points	0.99914	8.5×10^{-4}

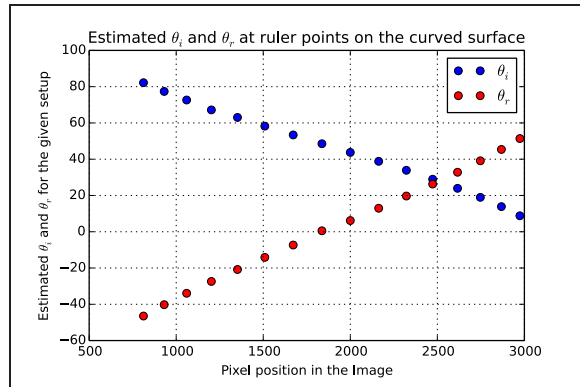


Figure 9. Calculated θ_i and θ_r as a function of pixel positions in the image

the Pearson's distances.

Computing θ_i and θ_r using θ_S

θ_i and θ_r were calculated using the θ_S values obtained from the θ_S model for the points (P) on the ruler image (refer Figure 5 and 4). Figure 9 shows the computed angles as a function of the pixel positions in the image. The pixel positions correspond to the points (P) on the ruler sample curved onto the cylinder. Looking at the plot (Figure 9), we can understand that θ_i and θ_r will change depending on the direction of the light source and the camera. The incident θ_i and reflection θ_r angles will therefore have the following relationship with respect to θ_S and θ_L angles.

For, $\theta_S < \theta_L : \theta_i < 0, \theta_S > \theta_L : \theta_i > 0$,

And for, $\theta_S < 0 : \theta_r > 0, \theta_S > 0 : \theta_r < 0$

Where, $\theta_S = 0$ is the normal to the sample surface at line (OC).

From the sample ruler used in the experiment, for the ruler points (P), θ_S remains greater than θ_L and therefore θ_i is positive, whereas θ_r changes from positive to negative at the pixel position 1837 which corresponds to the ruler point (P) approximately on the normal to the sample.

Conclusion

In this paper we have presented a geometrical method to estimate the incident θ_i and reflection θ_r angles and a measurement setup which can be used to goniometrically measure homogeneous flexible object materials/substrates using an image based technique at a relatively faster speed. The proposed angle estimation model estimates the incident and reflection angles for the light information collected using a camera sensor array. The results obtained using the ruler sample, show that the geomet-

rical method corrects for the geometrical distortion caused due to the sample curvature. This method therefore can be used in measurement setups similar to the one proposed in this paper for BRDF measurements of such samples [17, 18], thus recording accurate spectral BRDF information and reflection properties of non-diffuse and gonio-chromatic materials. The number of incident and reflection angles at which the reflection information is to be recorded depends on the camera resolution and sample curvature.

The model and measurement setup can also be used in packaging industry to perform online gonio-metric measurements during material reproduction process to estimate the incident and reflection angles of homogeneous flexible object materials, when measuring light incident and reflected from such sample at different angles.

Future work

However, some constraints can be seen in the setup as listed below, which remains further challenges to be addressed in this field of research.

- The setup can be used on flexible objects only (for example paper substrates, thin card boards, etc) only. Samples which are flat rigid materials (like wood) can not be measured using the proposed setup.
- For non-diffuse glossy materials, image captured in a single shot for a given camera exposure/shutter speed will not be sufficient due to limited dynamic range of the camera sensor, non-diffuse reflections from the object due to its material properties, and illumination. In order to capture the complete dynamic range of non-diffuse objects more than one exposure/shutter speed settings are required. High dynamic range (HDR) image will therefore be required to capture the reflected light information from the non-diffuse sample.
- The object surface should be homogenous in nature. Non-homogenous samples will be difficult to measure as the information is recorded spatially.

Acknowledgments

We would like to thank and acknowledge the support of Associate Professor Peter Nussbaum for his suggestions and guidance in writing this paper, discussions with Prof. Jon Yngve Hardeberg, Associate Professor Marius Pedersen and PhD researcher Ping Zhao at the Colourlab.

References

- [1] Christian. Eugène. Measurement of "total visual appearance": a cie challenge of soft metrology. In *12th IMEKO TC1 and TC7 Joint Symposium on Man, Science and Measurement*, pages 61 – 65, Annecy, France, September 2008.
- [2] C. S. McCamy. Observation and measurement of the appearance of metallic materials. part 1. macro appearance. *Journal*, 1996.
- [3] *Appearance Measurements of Goniochromatic Colours*, number ISBN 978-1-4716-6869-2, Edinburgh, UK, April 2012. 3rd International Conference on Appearance.
- [4] R. G. W. Hunt. *Measuring Color*. Fountain Press, 3 edition, 1998.
- [5] A. Takagi, S. Sato, and G. Baba. Prediction of spectral reflectance factor distribution of color-shift paint finishes, 2007.
- [6] Eric. Kirchner and Cramer. Werner. Making sense of measurement geometries for multi-angle spectrophotometers, 2012.
- [7] CIE15.2. Colorimetry. CIE standard, 2004.
- [8] ISO5-4. Photography and graphic technology - density measurements: Geometric conditions for reflection density. ISO standard, 2009.
- [9] Maria. E. Nadal and Edward. A. Early. Color measurements for pearlescent coatings, 2004.
- [10] C. S. McCamy. Observation and measurement of the appearance of metallic materials. part ii. micro appearance, 1998.
- [11] Katharina. Kehren, Philipp. Urban, Edgar. Dörsam, and Andreas. Höpe. Performance of multi-angle spectrophotometers. AIC, 2011.
- [12] G. Baba. Gonio-spectrophotometry of metal-flake and pearl-mica pigmented paint surfaces. In *Proceedings of the fourth Oxford conference on spectrophotometry*, pages 79–86. SPIE, 2003.
- [13] Jan J. Koenderink Rong Lu and Astrid M. L. Kappers. Optical properties (bidirectional reflection distribution functions) of velvet. *Applied Optics*, 37(25):5974 – 5984, September 1998.
- [14] K. Kehren. *Optical Properties and Visual Appearance of Printed Special Effect Colors*. PhD thesis, Technischen Universität Darmstadt, Darmstadt, Germany, April 2013.
- [15] Stephen R. Marschner, Stephen H. Westin, Eric P. F. Lafortune, Kenneth E. Torrance, and Donald P. Greenberg. Image-based brdf measurement including human skin. In *10th Eurographics Workshop on Rendering*, pages 139 – 152, 1999.
- [16] S. Tominaga and N. Tanaka. Estimating reflection parameters from a single color image. *IEEE Computer Graphics and Applications*, 20(5):58 – 66, 2000.
- [17] Duck Bong Kim, Kang Su Park, Kang Yeon Kim, and Kwan H. Lee. High-dynamic-range camera-based directional reflectance distribution function measurement system for isotropic materials. *Optical Engineering*, 48(9)(093601):09360101 – 09360111, September 2009.
- [18] Duck Bong Kim, Myoung Kook Seo, Kang Yeon Kim, and Kwan H. Lee. Acquisition and representation of pearlescent paints using an image-based goniospectrophotometer. *Optical Engineering*, 49(4) (043604):04360401 – 04360413, April 2010.

Author Biography

Aditya Sole completed his bachelors from PVGs College of Engineering and Technology, Pune University, India in year 2005. In 2007 he completed his MSc in Digital Colour Imaging from London College of Communication, University of the Arts, London, UK. From 2008 till 2012 he worked as a Laboratory Engineer at the Norwegian Colour and Visual Computing Laboratory, Gjøvik University College, Gjøvik, Norway. Since 2012 he is working as a Project Manager for the EU funded CP7.0 project and as a PhD researcher at the Colourlab.